miR-29a/b cluster suppresses high glucose-induced endothelial-mesenchymal transition in human retinal microvascular endothelial cells by targeting Notch2

JIAYU ZHANG, YUE ZENG, JIAWEI CHEN, DAQIU CAI, CHENGWEI CHEN,
SIFANG ZHANG and ZHENGUO CHEN

Department of Ophthalmology, The Third Affiliated Hospital of Wenzhou Medical University,
Rui'an, Zhejiang 325200, P.R. China

Abstract. Several studies have previously reported that endothelial cells contributed to pathological fibrosis in proliferative diabetic retinopathy (PDR) through endothelial-mesenchymal transition (EndMT); however, the precise mechanism of this interaction has not been completely elucidated. The present study investigated the expression of microRNA (miR)-29a/b cluster in human retinal microvascular endothelial cells (HRMECs) and examined its functional role in high glucose (HG)-induced EndMT. HRMECs were exposed to glucose at concentrations of 5, 15, 30 and 50 mM for 7 days and reverse transcription-quantitative polymerase chain reaction, western blotting and immunofluorescence were conducted to determine the expression of genes associated with miR-29a/b and EndMT. A luciferase reporter gene assay was also performed to confirm the association between miR-29a/b and neurogenic locus notch homolog protein 2 (Notch2). The expression levels of miR-29a/b, and endothelial markers vascular endothelial cadherin and cluster of differentiation 31 were decreased, whereas the expression levels of Notch2 and mesenchymal markers, including α-smooth muscle actin, fibroblast-specific protein 1 (also named S100 calcium binding protein A4, S100A4), fibronectin and SNAI1 were increased in HRMECs under HG (30 nM) conditions. In addition, Notch2 was identified as a target of miR-29a and miR-29b. Overexpression of miR-29a/b downregulated the expression of Notch2 and subsequently suppressed HG-induced EndMT. Taken together, the results of the present study revealed that the miR-29/Notch2 signaling pathway may participate in the regulation of HG-induced EndMT, and may serve as a potential molecular target during fibrosis in PDR.

Introduction

Diabetic retinopathy (DR) is the most common and serious complication of diabetes mellitus (DM) and is a major vision-threatening eye disease in the working-age population (1). Despite a new generation of medications and modern vitreoretinal microsurgery in clinical treatments, the prevalence of DR has still risen dramatically over the last two decades (2). Therefore, further understanding of the pathogenesis of DR is required in order to improve the presently available clinical therapies.

Proliferative DR (PDR) is the advanced, sight-threatening stage of DR characterized by ischemia-induced pathological preretinal neovascularization and uncontrolled production of extracellular matrix (ECM) proteins associated with the outgrowth of epiretinal fibrovascular membranes (FVMs) at the vitreoretinal interface (3). An increasing amount of evidence has suggested that endothelial cells may undergo endothelial-mesenchymal transition (EndMT) under high glucose (HG) stimulation, which contributes to pathological fibrosis in PDR (4-6). EndMT is a complex biological process in which endothelial cells lose their specific markers, including cluster of differentiation 31 (CD31) and vascular endothelial (VE)-cadherin, and express higher levels of mesenchymal markers including α-smooth muscle actin (α-SMA), fibroblast-specific protein 1 (FSP1) and fibronectin (FN) (7,8). A more comprehensive understanding of the molecular mechanisms involved in the EndMT process may be used to provide a novel therapeutic approach to attenuate the formation of FVMs associated with PDR.

MicroRNAs (miRNAs/miRs) are small noncoding regulatory RNA molecules, ~18-22 nucleotides in length, which

post-transcriptionally regulate gene expression by binding the 3'-untranslated regions (3'-UTRs) of target mRNAs to repress their translation or decrease their stability (9). Previous studies have reported that a number of miRNAs, including miR-21 (10), miR-23b-3p (11), miR-195 (12) and miR-126 (13), may be involved in the development of DR. Our recent studies revealed that the expression level of the miR-29a/b cluster decreased in the retina tissue of diabetic rats, which may serve as an important biomarker in DR (14,15). An increasing amount of evidence has suggested that the miR-29 family could serve a role in the development of fibrosis of multiple organs, including renal, pulmonary and cardiac fibrosis (16-18). Therefore, the current study hypothesized that modulating the miR-29a/b cluster may provide a novel therapeutic strategy for fibrosis associated with PDR.

In the present study, human retinal microvascular endothelial cells (HRMECs) were used to elucidate the potential involvement of the miR-29a/b cluster in HG-induced EndMT. It was demonstrated that the expression level of miR-29a/b was decreased in HG-treated HRMECs, and overexpression of miR-29a/b inhibited the EndMT of HRMECs induced by HG. Further mechanistic studies indicated that neurogenic locus notch homolog protein 2 (Notch2) was a direct target of miR-29a/b and was involved in the progression of EndMT.

Materials and methods

Cells culture. Primary HRMECs isolated from a single donor eye were purchased from Cell Systems (Kirkland, WA, USA) and cultured in endothelial basal medium (Lonza Group, Ltd., Basel, Switzerland) supplemented with 10% fetal bovine serum, endothelial cell growth supplements (EGM SingleQuots; Lonza Group, Ltd.) and 1% penicillin/streptomycin (Invitrogen; Thermo Fisher Scientific, Inc., Waltham, MA, USA). All cultures were incubated at 37°C in a 5% CO_2 humidified atmosphere. Cells at passage 3-6 were used for subsequent experiments.

Cell stimulation. HRMECs were cultured in conditioned medium with various concentrations of D-glucose (Sigma-Aldrich; Merck KGaA, Darmstadt Germany) and were treated in 6 groups with the following for 7 days: 0 mM glucose, 5 mM glucose [serving as the normal glucose (NG) group], 15 mM glucose, 30 mM glucose (HG group), 50 mM glucose and 5 mM glucose + 25 mM mannitol (serving as the osmotic control). Cells were subsequently stimulated with HG or osmotic control for either 1, 3, 5 or 7 days. In certain experiments, a selective inhibitor of endogenous transforming growth factor-β (TGF-β) signaling (SB431542; 10 μM; Sigma-Aldrich; Merck KGaA) was added to cultures 1 h prior to treatment with NG or HG.

Cell transfection. HRMECs were seeded in six-well plates at a density of $1x10^5$ cells/well for 24 h. A total of 100 nM miR-29a and miR-29b mimics or inhibitors, and non-targeting control (NC) were subsequently transfected into cells using Lipofectamine® 2000 (Invitrogen; Thermo Fisher Scientific, Inc.). All miRNA mimics, inhibitors and miR-NC oligonucleotides were purchased from Guangzhou RiboBio Co., Ltd. (Guangzhou, China), the sequences of

which are listed in Table I. The pcDNA-enhanced green fluorescent protein (EGFP) vector with Notch2 cDNA (pcDNA-Notch2) and the blank pcDNA-EGFP plasmids (pcDNA) were purchased from Shanghai GeneChem Co., Ltd. (Shanghai, China). 1 mg pcDNA-Notch2 expression plasmid or blank pcDNA plasmid were transfected into HRMECs ($5x10^6$ cells/well) and the mock group was untransfected. At 24 h following transfection, HRMECs were washed with PBS and recorded using a laser-scanning confocal microscope (LSM710; Carl Zeiss AG, Oberkochen, Germany) to evaluate the transfection efficiency. Four images were obtained per well in two channels: HRMECs body and GFP. Transfection efficacy was calculated manually using the following formula: % transfection efficacy = green fluorescent cell number/cell number x100.

Reverse transcription-quantitative polymerase chain reaction (RT-qPCR). Total RNA was extracted from HRMECs using TRIzol® reagent (Invitrogen; Thermo Fisher Scientific, Inc.). The RNA quality was measured using a NanoDrop 2000 spectrophotometer (Thermo Fisher, Scientific, Inc.). For the detection of mRNA expression, cDNA was synthesized with 1 μg of total RNA using an iScript™ cDNA synthesis kit (Bio-Rad Laboratories, Inc., Hercules, CA, USA) according to the manufacturer's protocol. qPCR analysis was performed using the ABI 7000 PCR instrument (Applied Biosystems; Thermo Fisher Scientific, Inc.) with SYBR Premix Ex Taq™ II (Takara Biotechnology Co., Ltd., Dalian, China). The reaction for mRNA was performed under the following conditions: 95°C for 1 min, and 40 cycles at 95°C for 5 sec and 60°C for 30 sec. For the detection of miR-29a and miR-29b, total cDNA was synthesized by using a miScript II RT kit (Qiagen GmbH, Hilden, Germany), under the following conditions: 37°C for 60 min, 95°C for 5 min and 4°C for 5 min. qPCR of miRNA expression was performed using a miScript SYBR Green PCR kit (Qiagen GmbH). The thermocycling conditions for miRNA was pas follows: 95°C for 15 min, followed by 40 cycles at 94°C for 15 sec, 55°C for 30 sec and 70°C for 30 sec. The relative amounts of mRNA and miRNA were calculated using the $2^{-\Delta\Delta q}$ method and normalized to β-actin and U6 small nuclear RNA, respectively (19). The sequences of the primers are presented in Table I.

Western blotting. HRMECs were lysed in RIPA lysis buffer and the protein was collected and quantified with a bicinchoninic acid assay kit (Beyotime Institute of Biotechnology, Shanghai, China). A total of 40 μg of protein from each sample were subjected to sodium dodecyl sulfate polyacrylamide gel electrophoresis (10% gel) and electrotransferred onto polyvinylidene fluoride membranes. Following blocking with 5% non-fat milk (Sigma-Aldrich) at room temperature for 2 h, the membranes were incubated with primary antibodies against Notch 1 (cat. no. ab8925; 1:1,000), Notch 2 (cat. no. ab8926; 1:1,000), Jagged 1 (cat. no. ab7771; 1:1,000) and β-actin (cat. no. ab8227; 1:5,000) (all from Abcam, Cambridge, UK) at 4°C for 16 h. The membranes were then incubated with horseradish peroxidase-conjugated secondary antibodies (cat. no. 14708 or 14709; 1:5,000; Cell Signaling Technology, Inc., Danvers, MA, USA) for additional 2 h at 25°C. Western blots were visualized using Western Lighting Plus-ECL (PerkinElmer, Inc.,

Table I. Sequences of microRNAs and primers used in the current study.

microRNA/primer name	Sequence (5'→3')
miR-29a mimic	UAGCACCAUCUGAAAUCGGUUA
miR-29b mimic	UAGCACCAUUUGAAAUCAGUGUU
miR-29a inhibitor	UAACCGAUUUCAGAUGGUGCUA
miR-29b inhibitor	AACACUGAUUUCAAAUGGUGCUA
miRNA NC	UUUGUACUACACAAAAGUACUG
U6-F	CTCGCTTCGGCAGCACA
U6-R	AACGCTTCACGAATTTGCGT
miR-29a-F	TAGCACCATTTGAAATCAGTTT
miR-29a-R	TGCGTGTCGTGGAGTC
miR-29b-F	AAAATATTTGGTTTTTATTAGGGT
miR-29b-R	CATAACCTCTTCCTTTACCATTAAA
Jagged 1 (*Homo sapiens*)-F	GTCCATGCAGAACGTGAACG
Jagged 1 (*Homo sapiens*)-R	GCGGGACTGATACTCCTTGA
Notch1 (*Homo sapiens*)-F	TGGACCAGATTGGGGAGTTC
Notch1 (*Homo sapiens*)-R	GCACACTCGTCTGTGTTGAC
Notch2 (*Homo sapiens*)-F	CTCTTCCGTATCCGCACCATCATG
Notch2 (*Homo sapiens*)-R	GAGCCATGCTTACGCTTTCG
VE-cadherin (*Homo sapiens*)-F	CTACCAGCCCAAAGTGTGTG
VE-cadherin (*Homo sapiens*)-R	GTGTTATCGTGATTATCCGTGA
FSP1 (*Homo sapiens*)-F	GCAACAGGGACAACGAGG
FSP1 (*Homo sapiens*)-R	CTGGGCTGCTTATCTGGG
FN (*Homo sapiens*)-F	GATAAATCAACAGTGGGAGC
FN (*Homo sapiens*)-R	CCCAGATCATGGAGTCTTTA
SNAI1 (*Homo sapiens*)-F	TTCCAGCAGCCCTACGAC
SNAI1 (*Homo sapiens*)-R	AGCCTTTCCCACTGTCCTC
β-actin (*Homo sapiens*)-F	CAAAGGCCAACAGAGAGAAGAT
β-actin (*Homo sapiens*)-R	TGAGACACACCATCACCAGAAT

F, forward primer; R, reverse primer; miR, microRNA; NC, nontargeting control; Notch, neurogenic locus notch homolog protein; FN, fibronectin; FSP1, fibroblast-specific protein 1; VE-cadherin, vascular endothelial cadherin; U6, U6 small nuclear RNA.

Waltham, MA, USA) and recorded using the Bio-Rad gel image analysis system (Bio-Rad Laboratories, Inc.). β-actin was used as the internal control.

Immunofluorescence. HRMECs were rinsed in 1X PBS and fixed with 4% paraformaldehyde at 25˚C for 30 min and permeated with 0.2% Triton X-100 (Beyotime Institute of Biotechnology) in PBS for 10 min. Following blocking with 5% goat serum (cat. no. C-0005; BIOSS, Beijing, China) for 30 min at 25˚C, fixed cells were incubated with a primary antibody against CD31 (cat. no. ab28364; 1:200) or α-SMA (cat. no. ab5694; 1:200) (both from Abcam) overnight at 4˚C. The cells were then washed three times with PBS and incubated with Alexa Fluor 488 AffiniPure goat anti-mouse IgG (cat. no. 115-545-062) or FITC-conjugated goat anti-rabbit IgG (cat. no. 111-095-144) (both from Jackson ImmunoResearch Laboratories, West Grove, PA, USA) at a dilution 1:200 for 1 h at 37˚C. Nuclei were counterstained with 1 mg/ml DAPI (cat. no. d1306; Invitrogen; Thermo Fisher Scientific, Inc.) for 5 min at 25˚C. The cells were then visualized under a laser-scanning confocal microscope (Carl Zeiss).

Luciferase reporter assay. The binding sites of miR-29a and miR-29b with Notch2 were predicted using the TargetScan program (http://www.targetscan.org/vert_72/). Wild-type (WT) 3'-UTR of the Notch2 gene containing the predicted miR-29a/b binding site and relevant mutant controls (MUT) were cloned into pGL3 vectors (Promega Corporation, Madison, WI, USA). HRMECs were co-transfected with 100 ng of pGL3-Notch2 3'-UTR or pGL3-Notch2-mut 3'-UTR reporter plasmid and 10 ng of *Renilla* luciferase expression plasmid pRL-TK (Promega Corporation), with 100 nM miR-29a/b mimics, inhibitors or miR-NC using Lipofectamine 2000 transfection reagent (Thermo Fisher Scientific, Inc.). Cells were harvested and lysed 48 h later and luciferase activity was determined using a Dual-Luciferase reporter assay kit (Promega Corporation). Firefly luciferase activity was normalized to that of *Renilla* luciferase.

Statistical analysis. All data are presented as the mean ± standard deviation and were analyzed using SPSS statistical software (version 21.0; IBM Corp., Armonk, NY, USA). The
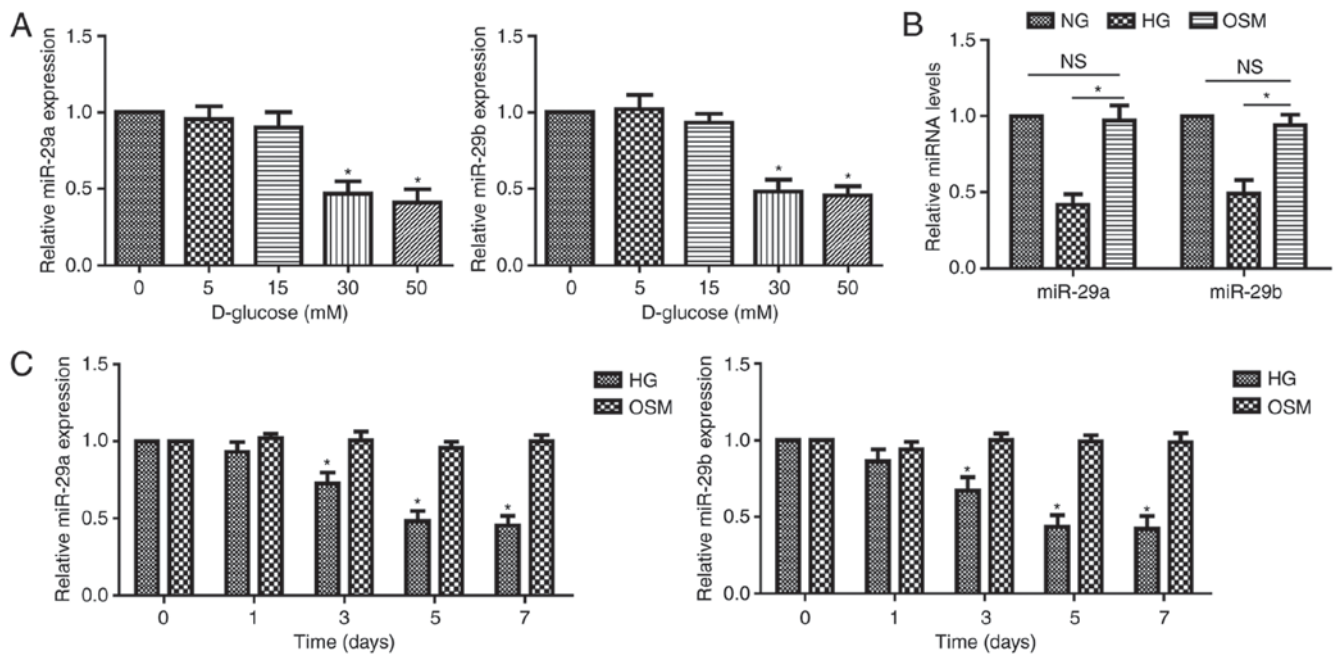
Figure 1. Expression pattern of miR-29a/b in HG-stimulated HMRECs. (A) RT-qPCR was used to determine the mRNA expression of miR-29a/b in HRMECs pretreated for 7 days with 5, 15, 30 and 50 mM of D-glucose. (B) RT-qPCR was used to determine the mRNA expression of miR-29a/b in HRMECs pretreated for 7 days with NG (5 mM), HG (30 mM) and OSM (5 mM glucose +25 mM mannitol). (C) RT-qPCR was used to determine the mRNA expression of miR-29a/b in HRMECs pretreated with HG or OSM for 1, 3, 5, or 7 days. Data are presented as the mean ± standard deviation from 3 different experiments, each performed in triplicate. Data were analyzed by one-way analysis of variance followed by Dunnett's post hoc test. *$P<0.05$ compared with the untreated group. HG, high glucose; NG, normal glucose; RT-qPCR, reverse transcription-quantitative polymerase chain reaction; miR, microRNA; OSM, osmotic control; HRMECs, human retinal microvascular endothelial cells.

differences were analyzed using Student's t-test for datasets containing two groups and one-way analysis of variance followed by Bonferroni or Dunnett's post hoc test for multiple group comparisons. $P<0.05$ was considered to indicate a statistically significant difference.

Results

HG induces a decrease in the expression of miR-29a/b in HRMECs. To clarify the effect of HG on the expression of miR-29a and miR-29b, HRMECs were cultured and treated with different concentrations of D-glucose (5-50 mM) for 7 days and HG (30 mM) for various times (1-7 days). The results of RT-qPCR analysis revealed that treatment with 30 mM glucose significantly decreased the expression levels of miR-29a and miR-29b in HRMECs (Fig. 1A). In addition, the expression of miR-29a/b was significantly lower in the HG group compared with that in the OSM group, but not different between the NG group and OSM group at 7 days following stimulation (Fig. 1B). HRMECs exhibited significantly decreased levels of miR-29a/b following exposure to HG for [3]3 days (Fig. 1C). These results indicated that HG could induce the decreased expression of miR-29a/b in HRMECs.

miR-29a and miR-29b inhibit HG-induced EndMT in HRMECs. To further investigate the effects of miR-29a and miR-29b in EndMT, miR-29a/b mimics and miR-NC were transfected into HRMECs. RT-qPCR confirmed that the expression of miR-29a/b was significantly increased in HRMCEs transfected with miR-29a/b mimics compared with cells transfected with the miR-NC (Fig. 2A). HRMECs

exhibited an elongated spindle-shaped phenotype following culture with HG for 7 days (Fig. 2B). Immunofluorescence and RT-qPCR demonstrated that the levels of the endothelial markers CD31 and VE-cadherin were decreased, while the levels of the mesenchymal markers α-SMA, FSP1, FN and SNAI1 were increased in the HG group when compared with NG group (Fig. 2B and C) (20). However, the overexpression of either miR-29a or miR-29b reversed low levels of endothelial marker as well as the high levels of these mesenchymal markers (Fig. 2B and C). These results suggested a direct role of miR-29a/b in HG-induced EndMT in HRMECs.

miR-29a and miR-29b target Notch2 to regulate its expression in HRMECs. Notch signaling has been suggested to serve a role in retinal vascular morphogenesis during development and in pathological angiogenesis associated with ocular diseases, including DR (21,22). A recent report confirmed that Notch2 functions as a regulator of myocardial fibrosis in diabetic cardiomyopathy (23). RT-qPCR and western blot analyses demonstrated that HG treatment increased the mRNA and protein expression of Jagged 1, Notch1 and Notch2 in HRMECs (Fig. 3A and B). The TargetScan program was subsequently used to investigate the potential association between the miR-29a/b cluster and the Notch signaling pathway, and identified Notch2 as a target for miR-29a and miR-29b (Fig. 3C). The luciferase reporter assays revealed that the introduction of either miR-29a or miR-29b in HRMECs significantly suppressed the reporter activity of the WT but not that of MUT Notch2 3'-UTR. However, an increase in the luciferase activity of WT 3'-UTR of Notch2 was observed following transfection with the miR-29a/b inhibitors (Fig. 3D).
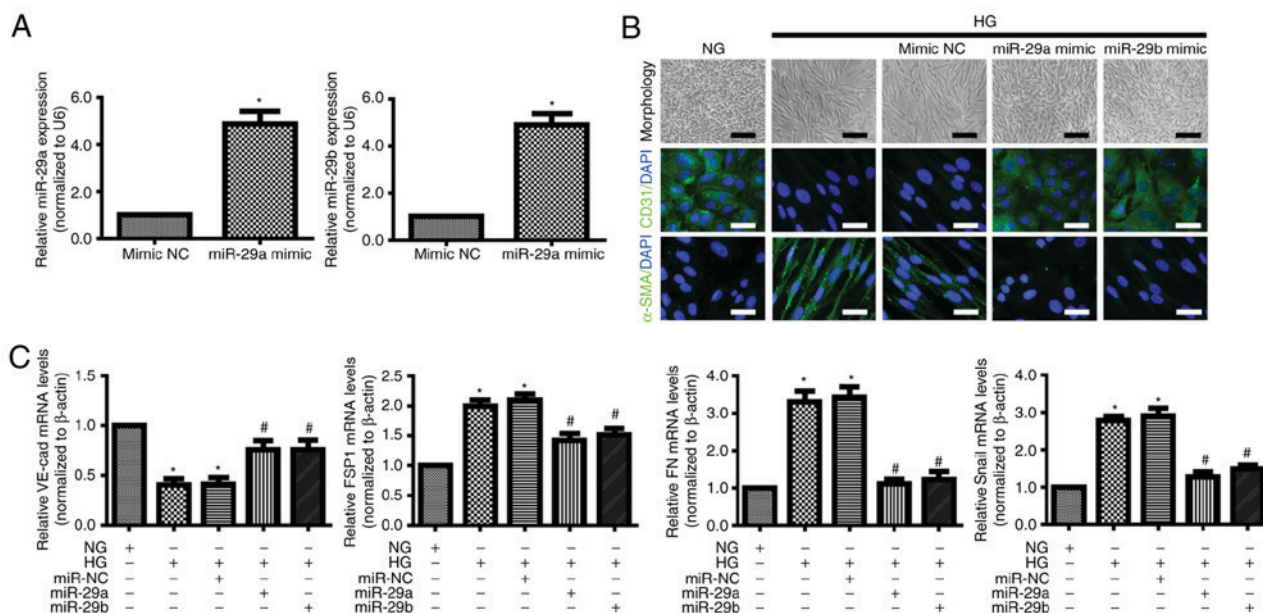
Figure 2. miR-29a/b overexpression inhibits HG-induced endothelial-mesenchymal transition of HRMECs. HRMECs were transfected with miR-NC, miR-29a mimic or miR-29b. (A) RT-qPCR analysis was performed to detect the expression of miR-29a and miR-29b. Data were analyzed using Student's t-test. P<0.05 compared with the mimic NC group. (B) Morphological alterations and expression of CD31 and α-SMA in HRMECs under NG (5 mM) and HG (30 mM) conditions for 7 days (black scale bar, 100 μm; white scale bar, 50 μm). (C) RT-qPCR was used to determine the mRNA expression of VE-cad, FSP1, FN and Snail in HRMECs under different conditions. Data were analyzed using one-way analysis of variance followed by Bonferroni post hoc test and are presented as the mean ± standard deviation from 3 different experiments, each performed in triplicate. *P<0.05 compared with the NG group; #P<0.05 compared with the HG group. HG, high glucose; NG, normal glucose; FSP1, fibroblast-specific protein 1; HRMECs, human retinal microvascular endothelial cells; miR, microRNA; NC, nontargeting control; VE-cad, vascular endothelial cadherin; FN, fibronectin; RT-qPCR, reverse transcription-quantitative polymerase chain reaction; α-SMA, α-smooth muscle actin; CD31, cluster of differentiation 31.

In addition, RT-qPCR analysis demonstrated that miR-29a/b overexpression markedly decreased Notch2 levels, which was further confirmed by western blotting. Reciprocally, the miR-29a/b silencing was accompanied by an increase in Notch2 expression (Fig. 3E). These results suggested that Notch2 is a direct target of miR-29a/b in HRMECs.

miR-29a and miR-29b suppress the HG-induced EndMT via the Notch2 signaling pathway in HRMECs. The present study further investigated whether Notch2 contributed to inducing EndMT following treatment with HG. EGFP was used to detect pcDNA-Notch2 plasmid transfection efficiency and the results demonstrated that the rate of fluorescent events was ~50% (Fig. 4A). RT-qPCR and western blot analyses revealed that transient Notch2 expression in HRMECs led to substantial upregulation of the Notch2 level (Fig. 4C). Co-transfection with miR-29a or miR-29b mimic and the Notch2 expression plasmid (but not the pcDNA-vector plasmid) could partly reverse the effect of miR-29a/b mimics on the expression of endothelial markers CD31 and VE-cadherin, and mesenchymal markers α-SMA, FSP1, FN and Snail. These were consistent with previous results and further demonstrated that the downregulation of miR-29a/b was concurrent with the upregulation of Notch2 during EndMT induced by HG in HRMECs (Fig. 4B and D). Therefore, the suppressed miR-29a/b levels appeared to be essential in inducing the upregulation of Notch2 in the EndMT process. Additionally, Notch2 overexpression alone or SB431542 pretreatment could alter the phenotype of HRMECs in NG and HG conditions (Fig. 4E). However, SB431542 pretreatment could not alter the phenotype of Notch2 overexpressed HRMECs in

HG conditions. Taken together, these results confirmed that miR-29a/b suppressed the HG-induced EndMT via the Notch2 signaling pathway, which is independent of TGF-β signaling.

Discussion

Endothelial dysfunction is the predominant manifestation in chronic diabetic complications including DR (24,25). Hyperglycemia induces endothelial injury by producing altered amounts of multiple proteins, which serve roles in EndMT (4-6). Cao *et al* (6) identified that glucose-induced EndMT in the retinal endothelial cells is mediated through TGF-β1 and is regulated by miR-200b. Abu *et al* (5) demonstrated that EndMT serves a role in creating myofibroblasts, which are responsible for the progression of fibrosis associated with PDR. Recently, Chang *et al* (4) confirmed EndMT in PDR epiretinal membranes obtained from patients undergoing *pars plana* vitrectomy and suggested that endothelin-1 served a role in promoting this transformative process. The results of the present study demonstrated that HG-induced a significant decrease in the expression of miR-29a and miR-29b in HRMECs, and further demonstrated that miR-29a/b overexpression inhibited HG-induced EndMT by targeting Notch2.

The miR-29 family, which includes miR-29a, miR-29b and miR-29c, has been demonstrated to regulate multiple physiological and pathological processes (26-28). For instance, miR-29a is involved in the pathogenesis of type 2 diabetes (29), and miR-29a overexpression counteracted the insulin inhibition of the phosphoenolpyruvate carboxykinase 2, mitochondrial gene by targeting phosphoinositide 3-kinase regulatory
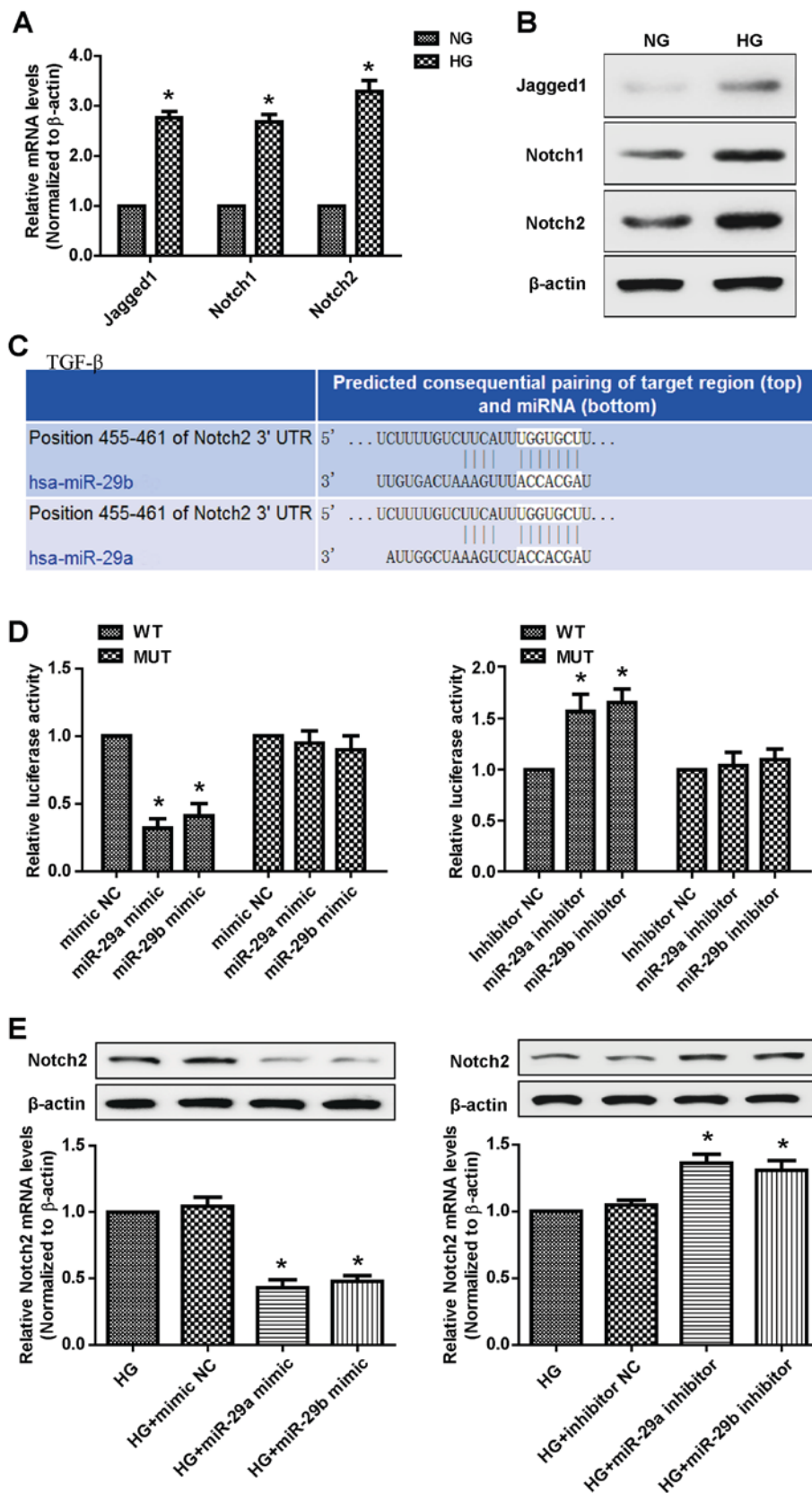
Figure 3. Notch2 is the target gene of miR-29a/b in HRMECs. The expression levels of Jagged 1, Notch1 and Notch2 were determined by (A) RT-qPCR and (B) Western blotting in HRMECs stimulated with HG (30 mM) for 7 days. Data were analyzed using Student's t-test. (C) Online TargetScan algorithm predicted that both miR-29a and miR-29b bound to the 3'-UTR of Notch2. (D) A luciferase reporter assay was performed to detect the relative luciferase reporter activity of the 3'-UTR of Notch2. Data were analyzed by one-way analysis of variance followed by Dunnett's post hoc test. *P<0.01 compared with the mimic NC group. (E) RT-qPCR and western blot analyses were used to detect the expression levels of Notch2 in HRMECs transfected with mimic/inhibitor NC, miR-29a mimic/inhibitor and miR-29b mimic/inhibitor. Data were analyzed by one-way analysis of variance followed by Dunnett's post hoc test and are presented as the mean ± standard deviation from 3 different experiments, each performed in triplicate. *P<0.01 compared with the HG group. Notch2, neurogenic locus notch homolog protein 2; HG, high glucose; HRMECs, human retinal microvascular endothelial cells; RT-qPCR, reverse transcription-quantitative polymerase chain reaction; UTR, untranslated region; miR/miRNA, microRNA; NC, nontargeting control; WT, wild-type; MUT, mutant control.
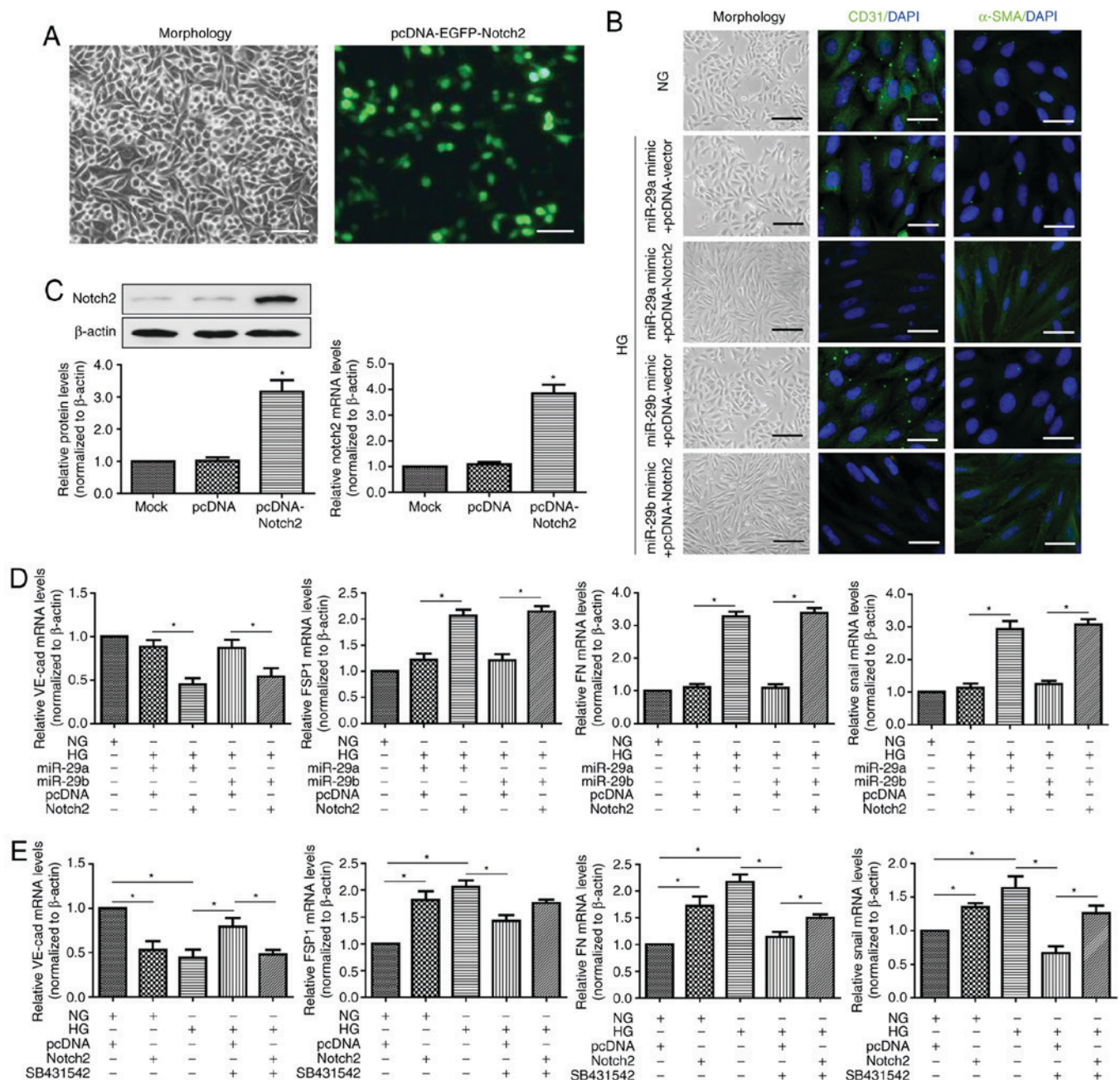
Figure 4. Notch2 overexpression rescues the inhibitory effect of miR-29a/b on endothelial-mesenchymal transition. (A) Transfection efficiency of pcDNA-Notch2 plasmid in HRMECs. Cells were analyzed under a fluorescence microscope after 48 h of transfection (scale bar, 100 μm). (B) Morphological alterations and expression of CD31 and α-SMA (black scale bar, 100 μm; white scale bar, 50 μm). (C) RT-qPCR and western blot analyses were performed to detect the expression of Notch2 in HRMECs transfected with blank pcDNA-vector and pcDNA-Notch2 plasmids. Mock group was set by adding transfection reagent only. Data were analyzed using one-way analysis of variance followed by Dunnett's post hoc test. *P<0.05 vs. the mock group. (D) mRNA expression of VE-cad, FSP1, FN and Snail in HRMECs co-transfected with miR-29a or miR-29b mimics and pcDNA-vector or pcDNA-Notch2 plasmid. Data were analyzed by one-way analysis of variance followed by Bonferroni post hoc test. Cells were incubated in NG (5 mM) or HG (30 mM) conditions for 7 days. (E) RT-qPCR was used to determine the mRNA expression of VE-cad, FSP1, FN and Snail in transfected HRMECs with or without SB431542 treatment. Cells were incubated with NG (5 mM) or HG (30 mM) conditions for 7 days. Data were analyzed by one-way analysis of variance followed by Bonferroni post hoc test and are presented as the mean ± standard deviation from 3 different experiments, each performed in triplicate. *P<0.05. Notch2, neurogenic locus notch homolog protein 2; HG, high glucose; NG, normal glucose; FSP1, fibroblast-specific protein 1; HRMECs, human retinal microvascular endothelial cells; EGFP, enhanced green fluorescent protein; α-SMA, α-smooth muscle actin; CD31, cluster of differentiation 31; FN, fibronectin; VE-cad, vascular endothelial cadherin; miR, microRNA; SB431542, transforming growth factor β1 inhibitor.

subunit p85α in HepG2 cells (30). In addition, inhibition of the expression of the miR-29a/b/c family via TGF-β1 promoted the synthesis and deposition of ECM components in cardiac or renal fibrosis (31,32). Our previous research revealed that the expression of miR-29a and miR-29b was decreased by HG stimulation and the downregulation of miR-29a/b exacerbated

DR by impairing the function of Müller cells (14,15). The present study, to the best of our knowledge, demonstrated for the first time that miR-29a/b in HRMECs may suppress HG-mediated EndMT. These results provide a potential novel mechanism for the antifibrosis effect of miR-29a/b on PDR and other chronic diabetic complications.

It has become increasingly apparent that the Notch signaling pathway may initiate EndMT, which contributes to the aggravation of cardiac fibrosis (23,33). A previous study demonstrated that Jagged 1-Notch interactions induced EndMT in microvascular endothelial cells (34). Therefore, the present study investigated the association between miR-29a/b and the Notch signaling pathway in EndMT physiopathology under HG conditions. RT-qPCR and western blot analyses revealed that the mRNA and protein levels of Jagged 1, Notch1 and Notch2 in the HG-treated HRMECs were significantly higher compared with the NG group. In addition, TargetScan predicted that miR-29a and miR-29b bound to the 3'-UTR of Notch2, with Luciferase reporter assays and western blotting further confirming that miR-29a and miR-29b negatively regulated the expression of Notch2. In addition, the overexpression of Notch2 reversed the inhibitory effect of miR-29a/b on EndMT, and was accompanied by the decreased expression of endothelial markers and the increased expression of mesenchymal markers. It has been demonstrated that TGF-β is a key inducer of EndMT (35) and that HG concentration increases the expression of TGF-β in various cells (36,37). However, the results of the current study revealed that pretreatment with the TGF-β inhibitor, SB431542, could not inhibit the HG-induced EndMT in Notch2 overexpressed HRMECs. Therefore, we hypothesize that the miR-29a/b cluster inhibits HG-induced EndMT of HRMECs by suppressing Notch2, irrespective of the status of the TGF-β signaling pathway.

In conclusion, data obtained in the present study indicated that a miR-29a/b/Notch2-mediated mechanism may be responsible for the process of EndMT in the context of PDR. Therapies based on controlling the expression of miR-29a/b may represent a promising direction for the treatment of PDR in the future.

Acknowledgements

Not applicable.

Availability of data and materials

All data generated or analyzed during this study are included in this published article.

Authors' contributions

JZ and ZC designed the study; JZ, YZ, JC, DC and CC performed the experiments; JZ and SZ analyzed the data; JZ, YZ and ZC drafted and revised the manuscript. All authors approved the final version for publication and agree to be accountable for all aspects of the work in ensuring that questions related to the accuracy or integrity of any part of the work are appropriately investigated and resolved.

Ethics approval and consent to participate

Not applicable.

Patient consent for publication

Not applicable.

Competing interests

The authors declare that they have no competing interests.

References

1. Cheung N, Mitchell P and Wong TY: Diabetic retinopathy. Lancet 376: 124-136, 2010.
2. Sabanayagam C, Yip W, Ting DS, Tan G and Wong TY: Ten emerging trends in the epidemiology of diabetic retinopathy. Ophthalmic Epidemiol 23: 209-222, 2016.
3. Michels RG: Proliferative diabetic retinopathy: Pathophysiology of extraretinal complications and principles of vitreous surgery. Retina 1: 1-17, 1981.
4. Chang W, Lajko M and Fawzi AA: Endothelin-1 is associated with fibrosis in proliferative diabetic retinopathy membranes. PLoS One 13: e0191285, 2018.
5. Abu El-Asrar AM, De Hertogh G, van den Eynde K, Alam K, Van Raemdonck K, Opdenakker G, Van Damme J, Geboes K and Struyf S: Myofibroblasts in proliferative diabetic retinopathy can originate from infiltrating fibrocytes and through endothelial-to-mesenchymal transition (EndoMT). Exp Eye Res 132: 179-189, 2015.
6. Cao Y, Feng B, Chen S, Chu Y and Chakrabarti S: Mechanisms of endothelial to mesenchymal transition in the retina in diabetes. Invest Ophthalmol Vis Sci 55: 7321-7331, 2014.
7. Pardali E, Sanchez-Duffhues G, Gomez-Puerto MC and Ten Dijke P: TGF-β-induced endothelial-mesenchymal transition in fibrotic diseases. Int J Mol Sci 18: E2157, 2017.
8. Piera-Velazquez S, Li Z and Jimenez SA: Role of endothelial-mesenchymal transition (EndoMT) in the pathogenesis of fibrotic disorders. Am J Pathol 179: 1074-1080, 2011.
9. Bartel DP: MicroRNAs: Genomics, biogenesis, mechanism, and function. Cell 116: 281-297, 2004.
10. Chen Q, Qiu F, Zhou K, Matlock HG, Takahashi Y, Rajala RVS, Yang Y, Moran E and Ma JX: Pathogenic Role of microRNA-21 in diabetic retinopathy through downregulation of PPARα. Diabetes 66: 1671-1682, 2017.
11. Zhao S, Li T, Li J, Lu Q, Han C, Wang N, Qiu Q, Cao H, Xu X, Chen H and Zheng Z: miR-23b-3p induces the cellular metabolic memory of high glucose in diabetic retinopathy through a SIRT1-dependent signalling pathway. Diabetologia 59: 644-654, 2016.
12. Mortuza R, Feng B and Chakrabarti S: miR-195 regulates SIRT1-mediated changes in diabetic retinopathy. Diabetologia 57: 1037-1046, 2014.
13. Qin LL, An MX, Liu YL, Xu HC and Lu ZQ: MicroRNA-126: A promising novel biomarker in peripheral blood for diabetic retinopathy. Int J Ophthalmol 10: 530-534, 2017.
14. Zhang J, Wu L, Chen J, Lin S, Cai D, Chen C and Chen Z: Downregulation of MicroRNA 29a/b exacerbated diabetic retinopathy by impairing the function of muller cells via forkhead box protein O4. Diab Vasc Dis Res 15: 214-222, 2018.
15. Zhang J, Chen M, Chen J, Lin S, Cai D, Chen C and Chen Z: Long non-coding RNA MIAT acts as a biomarker in diabetic retinopathy by absorbing miR-29b and regulating cell apoptosis. Biosci Rep 37: BSR20170036, 2017.
16. He Y, Huang C, Lin X and Li J: MicroRNA-29 family, a crucial therapeutic target for fibrosis diseases. Biochimie 95: 1355-1359, 2013.
17. Cushing L, Kuang P and Lu J: The role of miR-29 in pulmonary fibrosis. Biochem Cell Biol 93: 109-118, 2015.
18. Zhang Y, Huang XR, Wei LH, Chung AC, Yu CM and Lan HY: miR-29b as a therapeutic agent for angiotensin II-induced cardiac fibrosis by targeting TGF-β/Smad3 signaling. Mol Ther 22: 974-985, 2014.
19. Livak KJ and Schmittgen TD: Analysis of relative gene expression data using real-time quantitative PCR and the 2(-Delta Delta C(T)) method. Methods 25: 402-408, 2001.
20. Perez L, Munoz-Durango N, Riedel CA, Echeverria C, Kalergis AM, Cabello-Verrugio C and Simon F: Endothelial-to-mesenchymal transition: Cytokine-mediated pathways that determine endothelial fibrosis under inflammatory conditions. Cytokine Growth Factor Rev 33: 41-54, 2017.

21. Chen X, Xiao W, Liu X, Zeng M, Luo L, Wu M, Ye S and Liu Y: Blockade of Jagged/Notch pathway abrogates transforming growth factor β2-induced epithelial-mesenchymal transition in human retinal pigment epithelium cells. Curr Mol Med 14: 523-534, 2014.
22. Dou GR, Wang L, Wang YS and Han H: Notch signaling in ocular vasculature development and diseases. Mol Med 18: 47-55, 2012.
23. Geng H and Guan J: MiR-18a-5p inhibits endothelial-mesenchymal transition and cardiac fibrosis through the Notch2 pathway. Biochem Biophys Res Commun 491: 329-336, 2017.
24. Sorrentino FS, Matteini S, Bonifazzi C, Sebastiani A and Parmeggiani F: Diabetic retinopathy and endothelin system: Microangiopathy versus endothelial dysfunction. Eye (Lond) 32: 1157-1163, 2018.
25. Kang H, Ma X, Liu J, Fan Y and Deng X: High glucose-induced endothelial progenitor cell dysfunction. Diab Vasc Dis Res 14: 381-394, 2017.
26. Schmitt MJ, Margue C, Behrmann I and Kreis S: MiRNA-29: A microRNA family with tumor-suppressing and immune-modulating properties. Curr Mol Med 13: 572-585, 2013.
27. Kriegel AJ, Liu Y, Fang Y, Ding X and Liang M: The miR-29 family: Genomics, cell biology, and relevance to renal and cardiovascular injury. Physiol Genomics 44: 237-244, 2012.
28. Fabbri M, Garzon R, Cimmino A, Liu Z, Zanesi N, Callegari E, Liu S, Alder H, Costinean S, Fernandez-Cymering C, et al: MicroRNA-29 family reverts aberrant methylation in lung cancer by targeting DNA methyltransferases 3A and 3B. Proc Natl Acad Sci USA 104: 15805-15810, 2007.
29. Kong L, Zhu J, Han W, Jiang X, Xu M, Zhao Y, Dong Q, Pang Z, Guan Q, Gao L, et al: Significance of serum microRNAs in pre-diabetes and newly diagnosed type 2 diabetes: A clinical study. Acta Diabetol 48: 61-69, 2011.
30. Pandey AK, Verma G, Vig S, Srivastava S, Srivastava AK and Datta M: miR-29a levels are elevated in the db/db mice liver and its overexpression leads to attenuation of insulin action on PEPCK gene expression in HepG2 cells. Mol Cell Endocrinol 332: 125-133, 2011.
31. Wang B, Komers R, Carew R, Winbanks CE, Xu B, Herman-Edelstein M, Koh P, Thomas M, Jandeleit-Dahm K, Gregorevic P, et al: Suppression of microRNA-29 expression by TGF-β1 promotes collagen expression and renal fibrosis. J Am Soc Nephrol 23: 252-265, 2012.
32. van Rooij E, Sutherland LB, Thatcher JE, DiMaio JM, Naseem RH, Marshall WS, Hill JA and Olson EN: Dysregulation of microRNAs after myocardial infarction reveals a role of miR-29 in cardiac fibrosis. Proc Natl Acad Sci USA 105: 13027-13032, 2008.
33. Zhou X, Chen X, Cai JJ, Chen LZ, Gong YS, Wang LX, Gao Z, Zhang HQ, Huang WJ and Zhou H: Relaxin inhibits cardiac fibrosis and endothelial-mesenchymal transition via the Notch pathway. Drug Des Devel Ther 9: 4599-4611, 2015.
34. Noseda M, McLean G, Niessen K, Chang L, Pollet I, Montpetit R, Shahidi R, Dorovini-Zis K, Li L, Beckstead B, et al: Notch activation results in phenotypic and functional changes consistent with endothelial-to-mesenchymal transformation. Circ Res 94: 910-917, 2004.
35. Yoshimatsu Y and Watabe T: Roles of TGF-β signals in endothelial-mesenchymal transition during cardiac fibrosis. Int J Inflam 2011: 724080, 2011.
36. Yu CH, Suriguga, Gong M, Liu WJ, Cui NX, Wang Y, Du X and Yi ZC: High glucose induced endothelial to mesenchymal transition in human umbilical vein endothelial cell. Exp Mol Pathol 102: 377-383, 2017.
37. Di Paolo S, Gesualdo L, Ranieri E, Grandaliano G and Schena FP: High glucose concentration induces the overexpression of transforming growth factor-beta through the activation of a platelet-derived growth factor loop in human mesangial cells. Am J Pathol 149: 2095-2106, 1996.